Journal of Engineering Research (Libya)

AN OPTIMIZATION COMPARISON BETWEEN TAGUCHI BASED GRA AND DFA FOR DISSIMILAR WELDING MADE BY GTAW

Saleh Suliman Saleh Elfallah

College of Mechanical Engineering Technology, Benghazi, Libya
Email: salehelfallah87@gmail.com
Received 13 February 2026; Revised 26 June 2026; Accepted 28 June 2026; Published 4 July 2026.

مقارنة تحسين الأداء بين طريقة تاجوشي لتحليل الارتباط الرمادي وطريقة تحليل دالة الرغبة للحام غير المتشابه باستخدام لحام القوس التنجستن بالغاز

صالح سليمان صالح الفلاح

كلية تقنية الهندسة الميكانيكية، بنغازي، ليبيا

الملخص

يُستخدم اللحام بين المعادن غير المتجانسة بشكل شائع باستخدام لحام قوس التنغستن بالغاز، ولا سيما لربط الفولاذ المقاوم للصدأ مع الفولاذ منخفض الكربون في تطبيقات مثل محطات توليد الطاقة، وتجميعات المبادلات الحرارية، وصناعة السيارات، وإنشاء خطوط الأنابيب. ومع ذلك، يُعد اللحام غير المتشابه عملية دقيقة وأكثر تعقيدًا من اللحام المتجانس، وذلك بسبب الاختلافات في الخواص الميكانيكية والمعدنية للمعادن الأساسية. تؤثر معلمات اللحام، مثل تيار اللحام، وسرعة اللحام، ومعدل تدفق غاز الحماية، ونوع معدن الحشو، تأثيرًا كبيرًا في جودة الوصلة الملحومة النهائية. ولذلك، فإن تحسين هذه المعلمات يُعد أمرًا ضروريًا لتحقيق أداء لحام موثوق. وفي التطبيقات الصناعية، تُستخدم تقنيات متعددة لتحسين معلمات اللحام، سواء كانت أحادية الهدف أو متعددة الأهداف، بما في ذلك تصميم التجارب (DoE) والأساليب المعتمدة على الذكاء الاصطناعي. تقارن هذه الدراسة بين تحليل الارتباط الرمادي المعتمد على طريقة تاجوشي (GRA) ودالة الرغوبية (DFA) بوصفهما تقنيتين لتحسين متعدد الأهداف في لحام قوس التنجستن للمعادن غير المتشابهة بين الفولاذ المقاوم للصدأ (AISI 304) والفولاذ منخفض الكربون (EN10130) وتشمل معلمات اللحام التي تم دراستها تيار اللحام، وتركيب غاز الحماية، وحجم معدن الحشو. وقد أظهرت النتائج أن تحليل الارتباط الرمادي و دالة الرغوبية خلص إلى أن الوصلة الملحومة التي تم إنتاجها باستخدام اعدادات المعلمات: 120 أمبير، وحشو لحام بقطر 2.5 مم، وغاز حماية أرجون نقي تمثل الإعداد الأمثل. كما أظهرت الطريقتان دقة أعلي لتنبؤ تحليل الارتباط الرمادي بصفر خطأ بينما تنبؤ دالة الرغبة بلغت 4.25 % والتي تجيز دقة مقبولة للتنبؤ.

الكلمات المفتاحية: لحام قوس التنجستن لحام، الخواص الميكانيكية، فولاذ مقاوم للصدأ، فولاذ منخفض الكربون، لحام غير متجانس، تحليل تاجوشي، تحليل الارتباط الرمادي، دالة الرغوبية.

Copyright © 2026 by Faculty of Engineering, University of Tripoli, Libya.
This work is licensed under a Creative Commons Attribution 4.0 International License, which permits unrestricted use, distribution, and reproduction in any medium, provided the original work is properly cited.

ABSTRACT

Dissimilar metal welding is commonly performed using Gas Tungsten Arc Welding (GTAW), particularly for joining stainless steel and low-carbon steel in applications such as power plants, heat exchanger assemblies, pipeline construction and, automobile manufacturing. However, dissimilar welding is a delicate and more challenging process than homogeneous welding due to differences in the mechanical and metallurgical properties of the base metals. Welding parameters such as welding speed, welding current, shielding gas flow rate, and filler metal type have a significant influence on the quality of the final weldment. Therefore, optimization of these parameters is essential to achieve reliable weld performance. In industrial practice, various single and multi-objective optimization techniques, including DoE and artificial intelligence based methods employed to optimize welding parameters. This study compares Taguchi-based GRA and DFA as multi-objective optimization techniques for GTAW dissimilar welding of AISI 304 stainless steel and EN10130 mild steel. The welding parameters investigated include welding current, shielding gas composition, and welding filler size. The results have shown that GRA and DFA have concluded that weldment with parametric combination of 120 A, 2.5 mm welding filler and pure Ar shielding gas has shown optimal setting. The Taguchi-based GRA exhibited 0 % prediction error for the optimal combination prediction indicating excellent and highly reliable model, while a concluded DFA error of 4.25 % validates the model accuracy as acceptable.

KEYWORDS: GTAW, mechanical properties, dissimilar welding, Taguchi, GRA, DFA.

INTRODUCTION

Dissimilar welding of metal is demanding in advanced technology due to its provision of unique advancement of combining dissimilar metal properties and therefore, the ability to increase the performance of structures and components [1]. However, joining dissimilar welding is more challenging than similar or homogenous welding owing to the differences in metallurgical and physical properties of the base metals [2]. Stainless steel and low-carbon steel are commonly included in dissimilar welding in industry in applications such as in construction, automation, oil and gas, power plants and ships [2], [3].

Gas tungsten arc welding (GTAW), also known as tungsten inert gas (TIG) is common in welding of aluminum, stainless steel, magnesium and titanium, since it provides advantages including narrow heat affected zone (HAZ), deeper penetration due to concentrated heat input, slag-free welds, all to which lead to higher quality welding. GTAW uses tungsten as an establishing arc electrode and an inert shielding gas such as argon to protect the weld from atmospheric oxidation, and welding filler to fill the weld [1].

The dissimilar welding of stainless steel especially 304 and low-carbon steel is well known in industry in applications that take advantages of the low cost of low-carbon steel and corrosion resistance of the stainless steel and when the transition in the mechanical properties and performance is required [1]. However, in order to achieve higher quality welds, it is vital to optimize the welding parameters such as welding current, speed and voltage, shielding gas flow rate and combination, and welding filler type and size [4]. For that the mechanical and metallurgical properties are influenced by such parameters [1].

Conventional trial-and-error experimentation for process parameter setting is inherently time-consuming, costly, and inefficient. In contrast, modern optimization techniques-particularly mathematical and metaheuristic [5] are used. There are several optimization techniques that analyze the process parameters and their influence and obtain the optimum combination for a desired output. Such as design of experiments (DoE) include full factorial, response surface methodology (RSM) and Taguchi method [6]. Other optimization techniques focus on multi-objective characteristics include grey relational analysis (GRA), desirability functional analysis (DFA) and Technique for Order Preference by Similarity to Ideal Solution (TOPSIS) [7]. Other technique that are capable of optimizing multi-objective output based on meta-heuristics algorithms include generic algorithm (GA), ant colony optimization (ACO), and particle swarm optimization algorithm (PSO) [8]. These techniques due to their ability to capture nonlinear relationships compared to conventional mathematical models are combined with artificial intelligence based approaches [9], [10]. ANN models require sufficiently large datasets for reliable training and validation to avoid overfitting [11].

Several studies have investigated the parametric optimization of GTAW dissimilar welding applying single-objective characteristics optimization techniques such as Taguchi and RSM, and multi-objective optimization such as DFA and GRA. Waziri et al. [12] employed response surface methodology (RSM) for optimizing GTAW parameters to the dissimilar welding of AISI 1008 low-carbon steel and A316 stainless steel. An optimum weldment tensile strength of 474 MPa was achieved at a welding speed of 45 mm/min, welding current of 160 A, and shielding gas flow rate of 20 l/min. The developed predictive models showed good agreement with experimental data, yielding correlation coefficients (R^2) of 0.9445 for tensile strength and 0.8872 for impact strength. In addition, welding speed and gas flow rate were identified as the most influential factors affecting impact strength, which reached a maximum value of 159.95 J. In a related investigation, Assefa et al. [13] studied the dissimilar welding of AISI 316 stainless steel and AISI 1020 mild steel using an L16 orthogonal array. Multi-objective optimization was carried out through desirability function analysis (DFA), resulting in an optimal parameter set comprising a welding current of 90 A, gas flow rate of 10 L/min, root gap of 2.5 mm, and ER309L filler metal. This combination produced a composite desirability value of 0.9387, with predicted weldment tensile strength and hardness values of 493.2 MPa and 86 HRB (172 HV), respectively. Confirmation experiments validated the optimization, yielding weldment tensile strength and hardness values of 498 MPa and 88 HRB (178 HV), corresponding to improvements of 0.96% and 2.27%. Similarly, Elfallah [14] reported a multi-objective optimization study on GTAW of S235JR mild steel based on an L8 orthogonal array. A Taguchi-based grey relational analysis (GRA) approach was adopted, leading to improvements of 3.01% in weldment tensile strength and 1.84% in weld hardness during confirmation testing compared with the predicted results. The confirmed weldment tensile strength and hardness values were 232 MPa and 82.5 HV, respectively. The optimal welding conditions consisted of a current of 170 A, a welding speed of 100 mm/min, and a V-groove joint configuration.

Tensile strength of weldments is the most frequently investigated mechanical property in GTAW welding studies, accounting for approximately 23% of reported research, followed by weld bead geometry (22%) and weld hardness (15%). Among the welding parameters, welding speed and welding current are the most commonly

examined variables. In contrast, parameters such as shielding gas and welding filler size composition have received comparatively less attention [15].

Several studies on GTAW dissimilar welding of low-carbon steel and stainless steel have considered different types of filler metals, including ER70S-6 [16], ER308 [17], and ER309L [18]. Among these, ER309L is particularly preferred for welding stainless steel to carbon steel due to its ability to reduce susceptibility to hot cracking [19]. In addition, it is more tolerant of differences in chemical composition and thermal properties between the base metals, which helps to limit dilution effects and reduce crack formation [20], [21].

Argon (Ar) and Ar-carbon dioxide (CO_2) shielding gas mixtures containing up to 20% CO_2 are commonly employed for welding low-carbon steel, whereas their application to stainless steel is more limited [22]. Argon, being an inert gas, provides effective shielding against atmospheric contamination; however, due to its relatively unstable arc characteristics, it is often mixed with other inert gases such as helium (He) or with active gases such as CO_2 [23]. The addition of CO_2 contributes to arc stabilization, enhances weld penetration, and reduces spatter, all of which promote improved mechanical properties of the weldment [22].

Despite the growing body of research on parametric optimization of GTAW dissimilar welding between low-carbon steel and stainless steel, several gaps remain in the literature. Most existing studies have focused on a limited set of welding parameters, with shielding gas composition and filler wire size receiving comparatively less attention relative to current and speed. Furthermore, few studies have conducted a direct comparative evaluation of multi-objective optimization techniques, specifically GRA and DFA, applied simultaneously to the same experimental dataset for this material combination. The influence of shielding gas mixture, particularly argon and CO_2 combinations, on the mechanical performance of EN10130/AISI 304 dissimilar welds also remains insufficiently characterized. These gaps highlight the need for a more comprehensive and comparative optimization study targeting this industrially relevant joint configuration.

Therefore, the objective of the present study is to investigate the effect of welding current, filler wire size, and shielding gas composition on the mechanical properties specifically weldment tensile strength and hardness of GTAW dissimilar welds between EN10130 low-carbon steel and AISI 304 stainless steel. Multi-objective optimization is performed through a comparative application of Taguchi-based grey relational analysis (GRA) and desirability function analysis (DFA), with the significance of individual parameters assessed using analysis of variance (ANOVA).

METHODOLOGY

Materials and Experimentation

The base metals selected for the GTAW process dissimilar welding experiments consisted of low-carbon steel EN10130 grade DC01, in accordance with the European standard, and austenitic stainless steel AISI 304, specified by the American Iron and Steel Institute (AISI). The welding process is performed by ER309L, with rod sizes; 3/32 in (~2.18 mm) and 1/8 in (~3.38 mm). The elemental composition of the base metals and the welding filler are summarized in Table (1) and the mechanical properties in Table (2). The shielding gas applied 100 % Ar and a mixture of 90 % Ar and 10 % CO_2. It's common

in local industry to apply a combination of 80% Ar and 20% CO_2 to weld mild steel, however, it's recommended for low-carbon steel and stainless steel dissimilar welding to apply a combination of 90% Ar and 10% CO_2 or 85% Ar and 15% CO_2. The role of CO_2 is vital as it provides wettability and necessary oxidation for low carbon steel in the weld [24]. The range of welding current was determined based on preliminary trial-and-error trials and findings from previous studies, whereas the welding voltage was automatically controlled within the range of 14-20 V.

Table 1: The elemental composition of the base metal and welding filler used in the experiment.

Component		Composition (%)									
		C	Mn	Mo	S	Ni	Cr	P	Si	Cu	Fe
Base metal	EN 10130[a]	0.12	0.60	0.02	0.04	-	0.02	0.04	0.55	-	Balance
	AISI 304[b]	0.07	2	0.03	0.03	8-10.5	17.5-19.5	0.05	1	0.20	Balance
Welding filler	AWS E309L[c]	0.04	0.5-2.5	0.75	0.03	12-14	22-25	0.04	1	0.75	Balance

[a] The composition is based on ASTM A1008/A1008M-24

[b] The composition is based on ASTM A240/A240M

[c] The composition is based on AWS A5.4/A5.4M:2016 (R2022)

Table 2: The tensile strength and hardness of base metal and filler material.

Component		Tensile properties			Hardness properties	
		Tensile strength (N/mm^2)	Yield strength (N/mm^2)	Elongation (%)	Vickers micro-hardness (HV)	Brinell hardness (HBW)
Base metal	AISI 304[a]	515	205	40	92HRBW	201
	EN 10130[b]	270-390	≤280	28	≤140	-
Welding filler	AWS E309L[c]	520 (75 ksi)	-	30	-	-

[a] The mechanical properties are based on ASTM A1008/A1008M-24

[b] The mechanical properties are based on ASTM A240/A240M

[c] The mechanical properties are based on AWS A5.4/A5.4M:2016 (R2022)

The welding operations, schematically illustrated in Figure (1), were performed at the Gulf Company for Oil and Gas Production in Benghazi by a certified welder. A Lincoln® Electric Invertec power source was used in manual mode, with the welding speed maintained at approximately 150 mm/min. The base metal plates, having a thickness of 3 mm, that is commonly represented in local industrial applications, were prepared and sectioned by a laser cutting machine into standard tensile test specimens. Specimen preparation followed the ASTM E8/E8M-22 standard, as shown in Figure (2) [25]. A square butt joint configuration without edge preparation was adopted, resulting in an estimated an average dilution of 60%.

Figure 1: Welding process at the Gulf Company for Oil and Gas Production, Benghazi, Libya.

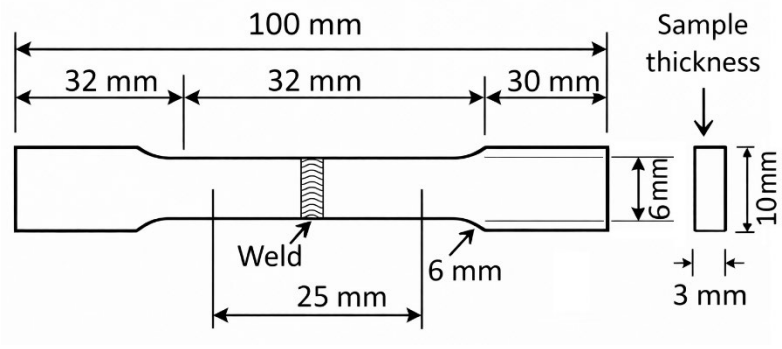

Figure 2: Tensile specimen specification.

Mechanical testing was carried out to evaluate weld performance. Tensile tests were conducted with two repetitions at the Libyan Advanced Occupational Center for Welding Technologies using an HST Hensgrand universal testing machine, as depicted in Figure (3). In addition, Vickers microhardness measurements were performed across the weldments using a hardness tester BMS Bulut Makina Sanayi®. A test with a dwell time of 10 s load of 500 g was applied, and the measurement positions at the fusion zone (FZ) are shown in Figure (4a). Figure (4b) shows the cross-sectional areas of the fusion zone, where a and c denote the base metal penetration zones on the EN10130 and AISI 304 sides, respectively, and b denotes the weld reinforcement, from which the dilution was calculated. The dilution (D) of the weld shown in Figure (4b) is 59.4% and is calculated using Equation (1),

$$D = \frac{a+c}{a+b+c} \times 100\% \quad (1)$$

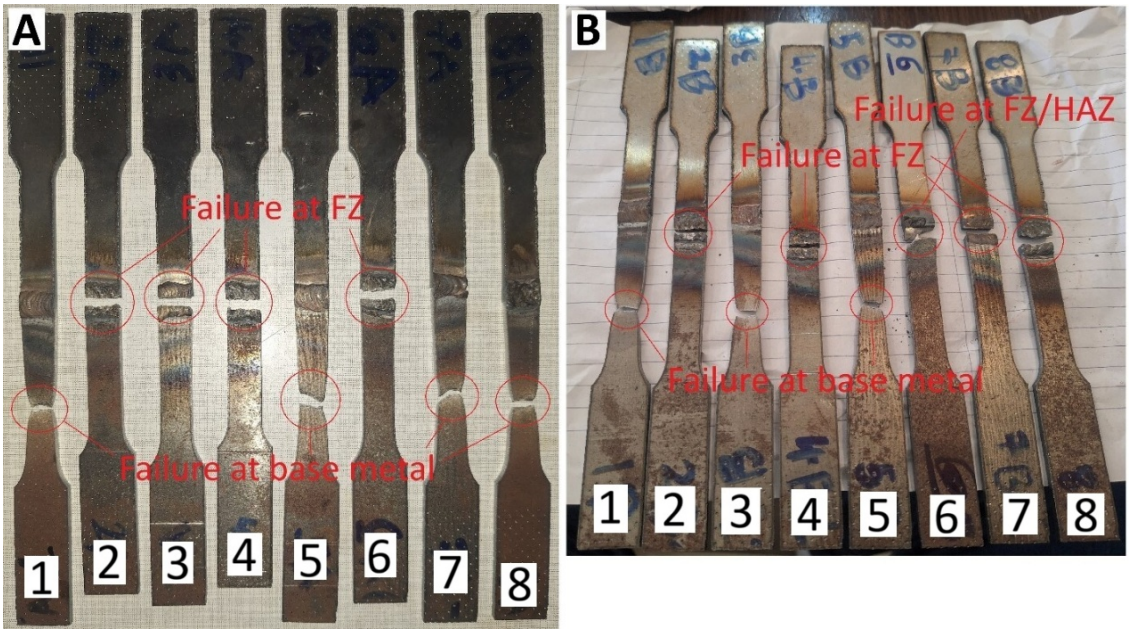

Figure 3: Following testing, tensile samples with two repetitions, A and B, displaying failure positions at the weld; FZ and heat affected zone (HAZ), and the base metal.

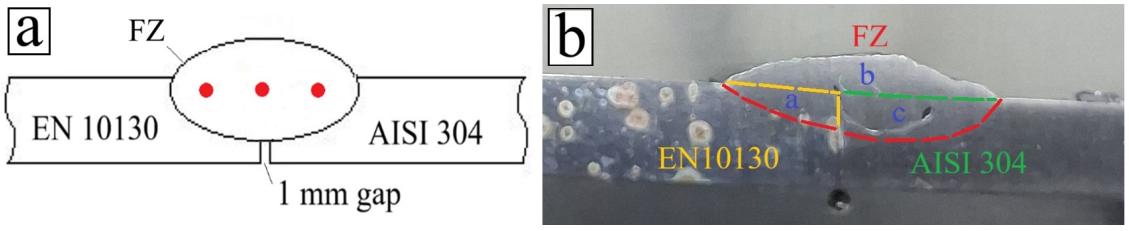

Figure 4: (a) The Vickers micro-hardness test positions at the FZ; (b) cross-section of weld presenting the penetration of FZ.

The experimental design based on Taguchi's orthogonal array involved three welding parameters, each include two levels. The total experiments led to eight experimental trials corresponding to an L8 array, as concluded in Table (3). ANOVA has evaluated statistically the significance of the parameters with the aid of Minitab 18® statistical software. The heat input of the GTAW process, expressed in J/mm, was calculated using Equation (2), assuming a thermal efficiency of 0.6, as recommended for GTAW [23],

$$Heat\ input = \frac{Voltage\,(V) \times Amperage\,(A) \times 60}{Travel\ speed\,(mm/min)} \times 0.6 \qquad (2)$$

GREY RELATIONAL ANALYSIS (GRA)

GRA is an analysis technique to solve multi-objective optimization by converting them into single grey relational grade (GRG). To achieve optimized weldment tensile strength and hardness or the responses, first, normalization was made to responses results generated by Taguchi based on larger-is-better for the responses to achieve optimum results. The GRG is an average of grey relational coefficient (GRC) that correspond to the response. Equation 3 represent the normalization of the response.

$$Y_i = \frac{y_i - min(y_i)}{max(y_i) - min(y_i)} \quad (3)$$

where, Y_i is the normalized response, i is the number of experimental data, yi is the response, and $min(\ y_i)$ and $max(\ y_i)$ are the minimum and maximum normalized values respectively. Second, compute the GRC by Equation 4,

$$\varepsilon_i = \frac{\Delta_{min} + \omega\Delta_{max}}{\Delta_i + \omega\Delta_{max}} \quad (4)$$

where, ε_i is GRC, Δ_i is the deviation among Y_i, ω is 0.5 (typical assumption), and Δ_{min} and Δ_{max} is the maximum and minimum values of Δ_i. Third, calculate the GRG by Equation 5,

$$G_i = \frac{1}{n}\sum \varepsilon_i \quad (5)$$

where, G_i is GRG and n is a total number of responses [14], [25].

DESIRABILITY FUNCTION ANALYSIS (DFA)

DFA is used to identify optimal process parameters for systems involving multiple performance characteristics by simultaneously optimizing more than one objective response [13]. In this work, DFA is adopted to achieve the concurrent optimization of weldment tensile strength and hardness. The step-by-step procedure of the DFA approach is outlined below:

- *Identification of responses*: the response variables selected for optimization are weldment tensile strength and weld hardness. For both responses, a larger-the-better criterion is adopted;
- *Establishment of bounds*: the lower (L_i) and upper (U_i) limits for tensile strength and hardness are defined based on the experimentally obtained data;
- *Formulation of desirability functions*: each response is converted into an individual desirability value (d_i) using Equation (6), where the desirability ranges from 0 (completely undesirable) to 1 (fully desirable);

$$d_i = \begin{cases} 0, & y_i \le L_i \\ \left(\frac{y_i - L_i}{U_i - L_i}\right)^{w_i}, & L_i < y_i < U_i \\ 1, & y_i \ge U_i \end{cases} \quad (6)$$

  where w_i is the weight factor reflecting the importance of the response.

- *Weight assignment and computation of composite desirability*: the weighting factors represent the relative importance of each response in the overall optimization process. In this study, weldment tensile strength and hardness are assumed to have equal significance in terms of structural integrity and service performance. Consequently, equal weights of 0.5 are assigned to tensile strength (w_{TS}) and hardness (w_H). Based on these weights, the overall composite desirability (D) is calculated using Equation (7) as follows:

$$D = d_{TS}^{0.5} \times d_H^{0.5} \quad (7)$$

- *Determination of the optimal process:* the combination of process parameters that produces the maximum composite desirability is identified as the optimal solution. The corresponding optimal response is predicted using the Taguchi

method, and the percentage error and absolute error are subsequently evaluated using Equation (8) as follows:

$$Percentage\ error\ (\%) = \left|\frac{Y_{actual} - Y_{predicted}}{Y_{predicted}}\right| \quad (8)$$

RESULTS AND DISCUSSION

Influence of Welding Parameters on Weldment Mechanical Performance

The tensile properties and Vickers micro-hardness results of the weldments corresponding to the conducted experiments are presented in Table (3) and Figures (5). The results demonstrate that welding current has a significant influence on weldment tensile strength, with higher tensile strength observed at a welding current of 120 A, as evident in experiments 5 to 8 in Figure (5). In contrast, the weldment micro-hardness exhibits noticeable fluctuations with no clear or consistent trend. The heat input based on Equation (2) was calculated 384 J/mm for experiments 1 to 4, and 576 J/mm for experiments 5 to 8 taking maximum welding voltage 20 V.

Interestingly, the use of pure argon shielding gas resulted in higher tensile strength compared with the mixed shielding gas (90% Ar + 10% CO_2), as illustrated in Figure (5). The enhanced tensile strength can be attributed to improved weld coherence and the occurrence of tensile failure in the low-carbon steel base metal, which possesses lower tensile strength (≥270 N/mm²) compared with the AISI 304 stainless steel base metal (≈505 N/mm²). This behavior is clearly observed in repeated tests for experiments 1, 3, 5, and 7, as shown in Figure (3). Again, no distinct trend is evident for micro-hardness across these experiments.

Table 3: The weldment tensile strength and weld micro-hardness.

Experiment No.	Welding current (A)	Welding filler size (mm)	Shielding gas composition	Tensile strength (MPa)	Yield strength (MPa)	Vickers micro-hardness (VHN)	Tensile strength/micro-hardness
1	80	2.5	100 % Ar	186.10	109.67	360.14	0.52
2	80	2.5	90 % Ar + 10 % CO_2	78.81	43.65	250.73	0.31
3	80	3.25	100 % Ar	123.69	68.47	264.52	0.47
4	80	3.25	90 % Ar + 10 % CO_2	49.83	46.57	312	0.16
5	120	2.5	100 % Ar	211.91	137.73	325.96	0.65
6	120	2.5	90 % Ar + 10 % CO_2	180.11	112.73	273.28	0.66
7	120	3.25	100 % Ar	198.16	124.28	261	0.73
8	120	3.25	90 % Ar + 10 % CO_2	189.42	125.78	248.52	0.80

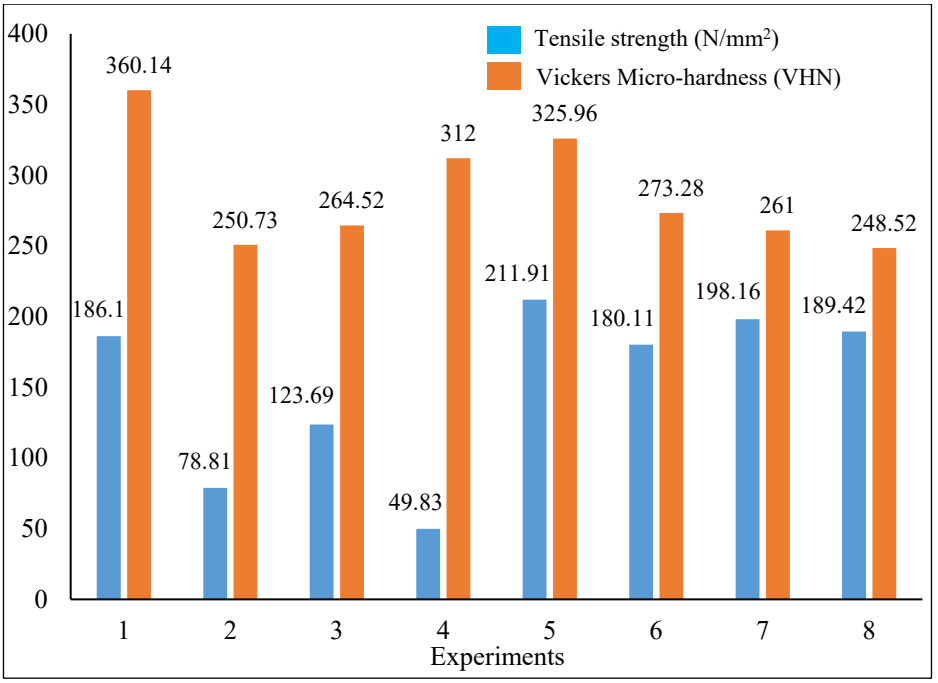

Figure 5: The weldments tensile strength and micro-hardness.

Among all results, experiment 5 exhibited the highest tensile strength of 211.91 MPa and yield strength of 137.55 MPa, corresponding to a welding current of 120 A, a filler size of 2.5 mm, and pure argon shielding gas. Furthermore, tensile failure in experiment 5 consistently occurred in the low-carbon steel base metal for both repetitions, as shown in Figure (3). Most of fails that occurred outside of weld area belong to weldments made using pure Ar shielding gas. The strong weld coherence in this case may also be related to the increased stiffness of the weld, reflected by its relatively high micro-hardness value of 325.96 VHN. Similarly, the highest weldment micro-hardness of 360.14 VHN recorded in experiment 1 may explain the tensile failure occurring in the EN10130 base metal rather than within the weld zone as seen in Figure (3).

The welding filler size appears to have a relatively minor effect on tensile strength but greater effect on micro-hardness. The tensile strength has reduced only 14.6 % in average at higher welding filler size compared to 43.8 % increase when increasing the current from 80 A to 120 A and 30.8 % reduction in tensile strength when using mixed shielding gas instead of pure Ar. Furthermore, the micro-hardness decreased by 10.3 % at filler size, similarly, when switching from pure Ar to mixed shielding gas caused a 10.5 % decrease in micro-hardness. This behavior can be attributed to increased filler deposition associated with larger filler diameters, which leads to higher heat input and enhanced molten metal volume in the weld zone, ultimately resulting in reduced micro-hardness [26].

The effect of heat input on the tensile strength and micr-hardness of weldments is evident when comparing the results of experiments 1-4 (384 J/mm) with those of experiments 5-8 (576 J/mm). The higher heat input at experiments 5 to 8 produced superior tensile and yield strengths improved by approximately 78% and 87%, for tensile strength and yield strength, respectively. This can be attributed to the greater thermal

energy the weld experience at higher welding currents, which promotes more complete fusion at the weld interface, and improves metallurgical bonding between the dissimilar base metals [27]. However, the micro-hardness exhibited an inverse trend, with the higher heat input for experiments 5 to 8 yielding a reduced weldment micr-hardness by 6.6 %.

This reduction in hardness at higher heat input is consistent with the slower cooling rates associated with greater thermal energy input, which promotes coarser grain growth in the fusion zone and heat-affected zone, thereby reducing hardness. This inverse relationship between hardness and tensile strength is further reflected in the tensile strength-to-hardness ratio, which was notably higher at increased heat input (576 J/mm) for experiments 5 to 8 scoring an increased ratio by 51.5 % in average, suggesting that the higher heat input favours improved ductility and load-bearing capacity of the weld joint over weld or FZ micro-hardness hardness.

TAGUCHI METHOD ANALYSIS FOR SINGLE-OBJECTIVE WELDING PARAMETERS

The signal to noise ratio (S/N) using the larger-is-better criterion was employed based on Taguchi analysis to maximize weldments tensile strength and micro-hardness. The welding current as presented in Figure (6) has shown higher S/N at 120 A followed by shielding gas at 100 % Ar, while the 2.5 mm welding filler had lower effect. That is consistent with welding current showing higher contribution with a F-value of 9.57, comprised about 62 %, as presented in Table (4). It indicates measurable and quantifiable effect of the welding current and shielding gas on tensile strength. The ANOVA and linear regression modeling were employed to evaluate the statistical significance of the process parameters. The results indicate that welding current has a statistically significant influence (0.036) on tensile strength ($p < 0.05$) as seen in Table (4), while shielding gas exhibits a moderate effect (0.091) and filler size is not statistically significant (0.379). The high coefficient of determination ($R^2 > 79\%$) confirms that the variation in tensile strength is predominantly explained by the process parameters rather than experimental noise.

The Vickers micro-hardness (VHN) evaluated using S/N indicates that shielding gas has the most influential effect, followed by welding filler size, while welding current exhibits the least influence on the micro-hardness as seen in Figure (6). The main effects plot for S/N ratios and means further reveal that Level 1 (100 % Ar) of shielding gas, Level 1 (2.5 mm) of welding filler size, and Level 1 (80 A) of welding current result in the highest micro-hardness values. The ANOVA as shown in Table (5) performed S/N ratios for weldment micro-hardness shows that none of the process parameters are statistically significant at the 95% confidence level ($p > 0.05$) with lower contribution of the parameters showing maximum F-value 1.11 (43 %) correspond to Shielding gas combination. This outcome is primarily attributed to the small experimental dataset.

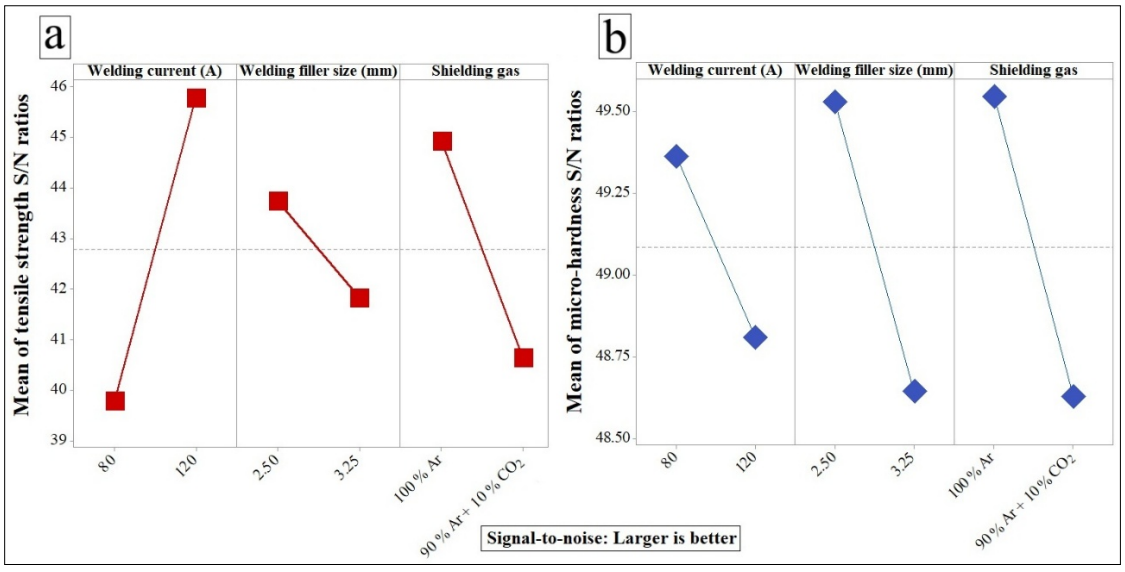

Figure 6: S/N ratio mean effect plot for weldments: (a) tensile strength and (b) micro-hardness.

Table 4: ANOVA for tensile strength S/N ratios.

Source	DF	Seq SS	Adj SS	Adj MS	F	R-eq
Welding current (A)	1	71.997	71.997	71.997	9.57	79.43 %
Welding filler size (mm)	1	7.363	7.363	7.363	0.98	
Shielding gas combination (l/mm)	1	36.826	36.826	36.826	4.89	
Residual Error	4	30.096	30.096	7.524		
Total	7	146.283				

Table 5: ANOVA for micro-hardness S/N ratios.

Source	DF	Seq SS	Adj SS	Adj MS	F	R-eq
Welding current (A)	1	0.611	0.611	0.611	0.40	38.96 %
Welding filler size (mm)	1	1.563	1.563	1.563	1.04	
Shielding gas combination (l/mm)	1	1.682	1.682	1.682	1.11	
Residual Error	4	6.042	6.042	1.511		
Total	7	9.899				

GREY RELATIONAL ANALYSIS (GRA) FOR MULTI-OBJECTIVE WELDING PARAMETERS

Table (6) presents the main effects plot of GRC, GRG, and ranking for weldment tensile strength and micro-hardness that correspond to the experiments. The normalized data indicate considerable variation in both tensile strength and micro-hardness across the experimental runs, reflecting the strong influence of welding parameters on weldment properties. The GRG was calculated for each response to evaluate each experiment's performance, and the GRG represents the overall performance index for multi-response optimization. The GRG indicates that experiment 1, which corresponds to weldment made at 80 A, 2.5 mm filler size, and pure Ar, achieved the highest GRG value of 0.963 and was ranked first, indicating favourable combination of tensile strength and micro-

hardness performance among the other experiments. Furthermore, experiment 5 came second with a close GRG value of 0.962 that corresponds to 120 A, a 2.5 mm filler size, and pure Ar. Moreover, Figure (7a) illustrate Taguchi's means effect plot showing 120 A, a 2.5 mm filler size, and pure Ar has the highest GRA means. This suggests that this welding parameters combination provide an optimal balance between weldment tensile strength and micro-hardness, which correspond to experiment 5. Overall, the experiments made at 120 A were ranked higher than the experiments at 80 A.

Table 6: The GRC and GRG tensile strength and weld micro-hardness.

Experiment no	Tensile strength (Normalized)	Micro-Hardness (Normalized)	Tensile strength GRC	Micro-hardness GRC	GRG	Rank
1	0.841	1	0.735	1.191	0.963	1
2	0.179	0.020	0.492	0.498	0.495	8
3	0.349	0.044	0.733	1.187	0.960	7
4	0.000	0.569	0.732	1.189	0.960	6
5	1	0.694	0.735	1.190	0.962	2
6	0.615	0.069	0.734	1.187	0.961	5
7	0.915	0.112	0.735	1.188	0.961	3
8	0.861	0	0.735	1.187	0.961	4

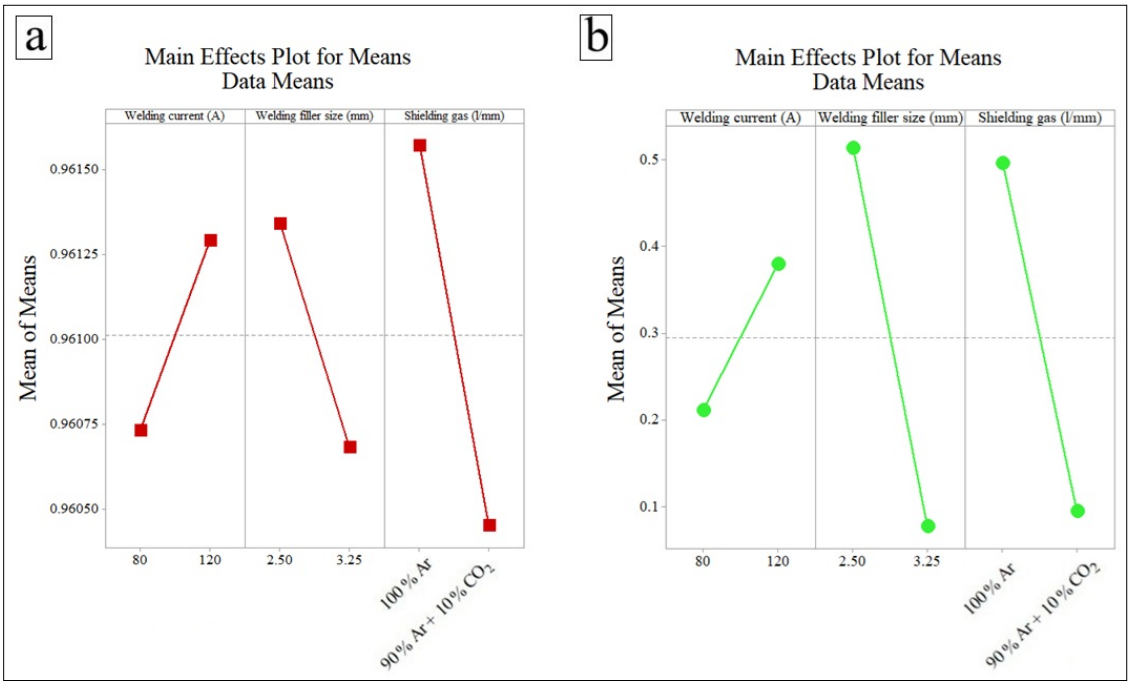

Figure 7: Means main effect plot for (a) GRA and (b) DFA.

DESIRABILITY FUNCTION ANALYSIS (DFA) FOR MULTI-OBJECTIVE WELDING PARAMETERS

Table (7) shows the individual desirability values for tensile strength and weld micro-hardness, along with the composite desirability index and corresponding ranks for each

experimental trial. The desirability is ranged from 0 to 1 is based on the degree to which each response satisfies the desired objective. The minimum tensile strength was set at 123.69 N/mm^2 to avoid abnormal results. The individual desirability has shown that experiment 5 has the maximum individual desirability of 1 as indicated in Table (7), indicating that it reached the target tensile strength. Similarly, micro-hardness desirability varied significantly, with experiment 1 demonstrating the highest value of 1, indicating superior weldment hardness. The composite desirability index represents a single metric of simultaneous multi-objective optimization of weldment tensile strength and micro-hardness. Table (7) indicates that experiment 1 has a record of 0.841 ranking 1st followed by experiment 5 (0.833) confirming initial approving combination of weldment tensile strength and micro-hardness similarly to GRA initial ranking. Nonetheless, the means main effect as presented in Figure (7b) shows that welding current 120 A, filler size 2.5 mm and pure Ar has optimal combination similar to the optimum combination resulted by GRG.

Table 7: Desirability index for weldment tensile strength and weld micro-hardness.

Experiment No.	Individual desirability		Composite desirability	Rank
	Tensile strength	Micro-hardness		
1	0.707	1	0.841	1
2	0	0.020	0	5
3	0	0.143	0	5
4	0	0.569	0	5
5	1	0.694	0.833	2
6	0.640	0.222	0.377	3
7	0.844	0.112	0.307	4
8	0.745	0	0	5

Validation Test

Table (8) presents the validation error of the optimum welding parameters. The predicted results shown in Table (8) are obtained using the Taguchi method, as expressed by Equation (9):

$$\eta_{opt} = \eta_m + \sum_{i=1}^{f}(\bar{\eta}_i - \eta_m) \quad (9)$$

where η_m is the mean of means, f is the number of parameters, $\bar{\eta}_i$ represents the mean of the means at the optimal level of factor i. The validation results reveal an identical percentage error of 0 % for GRA and 4.25 % DFA. Both optimization approaches agree on the optimal parameter levels of 120 A current and 100 % Ar as shielding gas, and the lower filler size of 2.5 mm, as shown in Table (7). The model predication accuracy for the GRA is considered excellent and it's most reliable, while for DFA the prediction error is considered acceptable, since it is within the acceptable threshold of 5%. The comparable error indicates superior validation reliability of the Taguchi-GRA optimization model. In general, the prediction error could be reduced by increasing the number of experiments runs for higher accuracy. Additionally, the Taguchi method has limitations in capturing nonlinear interactions, particularly with dissimilar welding processes.

Table 8: Optimal welding parameters validation error.

Optimal combination	Actual		Predicted		Validation error	
	GRA	DFA	GRA	DFA	GRA	DFA
120 A, 2.5 mm, 100 % Ar	0.962	-	0.962	-	0.0 %	-
120 A, 2.5 mm, 100 % Ar	-	0.833	-	0.797	-	4.26 %

CONCLUSION

GRA and DFA were successfully applied for multi-objective optimization of Gas Tungsten Arc Welding (GTAW) dissimilar joints between mild steel EN10130 and stainless steel AISI 304, considering weldment tensile strength and weld micro-hardness. The welding parameters investigated included welding current (80 A and 120 A), shielding gas composition (pure Ar and 90/10 Ar-CO_2), and welding filler sizes (2.5 mm and 3.25 mm). The study concluded the following:

- The weldment tensile strength increased with higher welding current (120 A) and the use of pure argon shielding gas. A maximum weldment tensile strength of 211.91 MPa and yield strength of 137.55 MPa were obtained at a welding current of 120 A, 2.5 mm filler size, and pure Ar shielding gas. The highest weldment micro-hardness value of 360.14 VHN was recorded for a weldment produced at 80 A, 2.5 mm filler size, and pure Ar;
- The samples experienced tensile test has failed in the weld area, the FZ and HAZ and at the low-carbon steel base metal mostly at weldment fabricated using pure Ar shielding gas. Most of fails that occurred outside of weld area associated with weldments made using pure Ar shielding gas;
- Based on multi-objective optimization, GRA identified 120 A welding current, 2.5 mm filler size, and pure Ar shielding gas as the optimal parameter combination that provides a balanced improvement in weldment tensile strength and micro-hardness. Similarly, DFA determined the same parameter combination as optimal;
- The GRA exhibiting a prediction error of 0 % for the optimal combination, which is considered excellent and proved highly model reliability, while it was 4.25 % for DFA that is considered acceptable and valid.
- It is acknowledged that this study is limited to mechanical performance the tensile strength and Vickers hardness, as the optimization response parameters. Microstructural characterization of the weld area, including the FZ and HAZ, as well as crystallographic and phase transformation analyses, were outside the defined scope of this work, which is focused on the methodological comparison between GRA Taguchi and DFA as multi-response optimization frameworks.

ACKNOWLEDGEMENTS

The author would like to thank his family for their encouragement and support. Sincere appreciation is extended to the staff of Libyan Advanced Occupational Center for Welding Technologies in Tajoura, Libya, and to the staff of the High Vocational Center of Casting in Tripoli, Libya, as well for their valuable assistance. An acknowledgment is given to College of Mechanical Engineering Technology in Benghazi, Libya.

DECLARATION OF CONFLICTING INTERESTS

The author declares no potential conflicts of interest with respect to the research, authorship, and/or publication of this article.

FUNDING

This author received no financial support for the research, authorship, and/or publication of this article.

DECLARATION OF GENERATIVE AI AND AI-ASSISTED TECHNOLOGIES IN THE WRITING PROCESS

The author has used ChatGPT-4 in language editing, however, the final writing was reviewed and verified by the author.

APPENDIX

Table 8: Nomenclature.

Symbol	Description
DF	Degree of freedom
Seq SS	Sequential Sum of Squares
Adj SS	Adjusted Sum of Squares
Adj MS	Adjusted Mean Square
F	F-value
P	Probability value
R^2	R-squared
GRG	Grey regression grade
GRC	Grey regression coefficient
GRA	Grey regression Analysis
DFA	Desirability function analysis
MPa	Mega Pascal
VHN	Vickers hardness number
ANOVA	Analysis of variance
DoE	Design of experiments
GTAW	Gas tungsten arc welding
FZ	Fusion zone
HAZ	Heat affected zone
Ar	Argon
CO_2	Carbon dioxide
J	Joule
mm	Millimeter

REFERENCES

[1] T. I. Ogedengbe, T. E. Abioye, and A. I. Ekpemogu, "Investigation of mechanical properties and parametric optimization of the dissimilar GTAW of AISI 304 stainless steel and low-carbon steel," *World J. Eng.*, vol. 15, no. 5, pp. 584–591, 2018, doi: 10.1108/WJE-12-2017-0412.

[2] E. Scutelnicu, M. Iordachescu, C. C. Rusu, D. Mihailescu, and J. L. Ocaña, "Metallurgical and mechanical characterization of low-carbon steel-stainless steel dissimilar joints made by laser autogenous welding," *Metals*, vol. 11, no. 5, p. 810, 2021, doi: 10.3390/met11050810.

[3] M. P. Prabakaran, G. R. Kannan, and R. Pandiyarajan, "Effects of welding speed on microstructure and mechanical properties of CO_2 laser welded dissimilar butt joints between low-carbon steel and austenitic stainless steel," *Adv. Mater. Process. Technol.*, vol. 8, suppl. 1, pp. 1–12, 2022, doi: 10.1080/2374068X.2020.1855960.

[4] H. Chen, B. Zhang, and T. Fuhlbrigge, "Welding process optimization methods: A review," *Trans. Intell. Weld. Manuf.*, vol. 3, no. 1, pp. 3–21, 2020, doi: 10.1007/978-981-13-8192-8_1.

[5] A. Das, R. Rai, B. Sasmal, K. G. Dhal, R. A. Khurma, and R. Saha, "Metaheuristic algorithms since 2020: Development, taxonomy, analysis, and applications," *Arch. Comput. Methods Eng.*, pp. 1–69, 2025, doi: 10.1007/s11831-025-10408-3.

[6] C. Aseibichin *et al.*, "Modeling and optimization of transesterification of Jatropha oil to fatty acid methyl ester: Application of response surface methodology (CCD) and Taguchi orthogonal method," *RSC Adv.*, vol. 14, no. 17, pp. 11784–11796, 2024, doi: 10.1039/D4RA01149J.

[7] S. Chihaoui, I. Meddour, M. Athmane Yallese, S. Belhadi, and K. Safi, "Comparative assessment between DFA, NSGA-II coupled with TOPSIS, GRA, and TOPSIS for multiobjective optimization of gray cast iron turning process using CBN insert," *Proc. Inst. Mech. Eng., Part E: J. Process Mech. Eng.*, vol. 238, no. 4, pp. 1765–1778, 2024, doi: 10.1177/09544089231194039.

[8] A. Banerjee, S. Pradhan, B. Misra, and S. Chakraborty, "A guide to meta-heuristic algorithms for multi-objective optimization: Concepts and approaches," *Appl. Multi-Objective Optim.*, vol. 1, pp. 1–19, 2024, doi: 10.1007/978-981-97-0353-1_1.

[9] C. C. Nwobi-Okoye, B. Q. Ochieze, and S. Okiy, "Multi-objective optimization and modeling of age hardening process using ANN, ANFIS and genetic algorithm: Results from aluminum alloy A356/cow horn particulate composite," *J. Mater. Res. Technol.*, vol. 8, no. 3, pp. 3054–3075, 2019, doi: 10.1016/j.jmrt.2019.01.031

[10] L. Perez Pozo, Z. F. Olivares, and A. O. Durán, "Optimization of welding parameters using a genetic algorithm: A robotic arm–assisted implementation for recovery of Pelton turbine blades," *Adv. Mech. Eng.*, vol. 7, no. 11, p. 1687814015617669, 2015, doi: 10.1177/1687814015617669.

[11] A. Kminus *et al.*, "Neural-Network-Based Approaches for Optimization of Machining Parameters Using Small Dataset, " *Materials*, vol. 15, no. 3, art. no. 700, 2022. DOI: 10.3390/ma15030700

[12] S. L. Waziri *et al.*, "Mechanical properties and microstructural characterizations of GTAW welded dissimilar joint of A316 stainless steel and AISI 1008 grade steel plates using RSM," *Proc. Inst. Mech. Eng., Part C: J. Mech. Eng. Sci.*, 2024, doi: 10.1177/09544062251368723.

[13] A. T. Assefa *et al.*, "Experimental investigation and parametric optimization of the tungsten inert gas welding process parameters of dissimilar metals," *Materials*, vol. 15, no. 13, p. 4426, 2022, doi: 10.3390/ma15134426.

[14] S. S. Elfallah, "Taguchi grey relational analysis of mechanical properties of structural steel welding made by gas tungsten arc welding," *Sci. J. Univ. Benghazi*, vol. 37, no. 1, pp. 37–47, 2024, doi: 10.37376/sjuob.v37i1.5938.

[15] A. Karpagaraj, K. Parthiban, and S. Ponmani, "Optimization techniques used in gas tungsten arc welding process–A review," *Mater. Today: Proc.*, vol. 27, pp. 2187–2190, 2020, doi: 10.1016/j.matpr.2019.09.093.

[16] M. Khan, M. W. Dewan, and M. Z. Sarkar, "Effects of welding technique, filler metal and post-weld heat treatment on stainless steel and mild steel dissimilar

welding joint," *J. Manuf. Process.*, vol. 64, pp. 1307–1321, 2021, doi: 10.1016/j.jmapro.2021.02.058.
[17] H. Hamdani, A. Akhyar, T. Rizwan, A. Sasmito, and H. A. Suhartono, "Mechanical and metallurgical properties of GTAW dissimilar welds between SUS304 and SA213T11 using ER308 filler metal: A preliminary study," *Adv. Sci. Technol. Res. J.*, vol. 19, no. 8, 2025, doi: 10.12913/22998624/204768.
[18] D. K. Singh *et al.*, "Investigation on the microstructure–mechanical property correlation in dissimilar steel welds of stainless steel SS 304 and medium carbon steel EN 8," *J. Manuf. Process.*, vol. 36, pp. 281–292, 2018, doi: 10.1016/j.jmapro.2018.10.018.
[19] C. Tembhurkar *et al.*, "Effect of fillers and autogenous welding on dissimilar welded 316L austenitic and 430 ferritic stainless steels," *J. Mater. Eng. Perform.*, vol. 30, no. 2, pp. 1444–1453, 2021, doi: 10.1007/s11665-020-05395-4.
[20] "ER70S-6 MIG welding wire data sheet," *Aircraft Materials*. [Online]. Available: https://www.aircraftmaterials.com/data/weld/er70s6.html. [Accessed: Mar. 24, 2025].
[21] "Welding dissimilar metals using 309 stainless steel," *ESAB*, 2024. [Online]. Available: https://esab.com/us/nam_en/esab-university/blogs/welding-dissimilar-metals-using-309-stainless-steel/. [Accessed: Mar. 24, 2025].
[22] T. Methong, "Influence of rare earth metal added to electrode on plasma characteristics in gas metal arc welding," Ph.D. dissertation, Osaka Univ., Osaka, Japan, 2018.
[23] G. Liu, X. Tang, Q. Xu, F. Lu, and H. Cui, "Effects of active gases on droplet transfer and weld morphology in pulsed-current NG-GMAW of mild steel," *Chinese J. Mech. Eng.*, vol. 34, no. 1, p. 66, 2021, doi: 10.1186/s10033-021-00583-2.
[24] "Welding dissimilar metals using 309 stainless steel," *ESAB*, 2026. [Online]. Available: https://www.esab.com/en-us/welding-dissimilar-metals. [Accessed: Feb. 6, 2026].
[25] A. B. Naik and A. C. Reddy, "Optimization of tensile strength in TIG welding using the Taguchi method and analysis of variance (ANOVA)," *Therm. Sci. Eng. Prog.*, vol. 8, pp. 327–339, 2018, doi: 10.1016/j.tsep.2018.08.005.
[26] A. A. Al-Azzawi *et al.*, "Effect of welding parameters on microstructure and mechanical properties of GMAW welded S275 steel welded zone," *Discover Materials*, vol. 4, art. no. 98, 2024. DOI: 10.1007/s43939-024-00169-4.
[27] M. Ş. Adin, "An investigation of the effect of GMAW and SMAW processes on mechanical and microstructural properties of welded E350 grade steel," *Scientific Reports*, vol. 15, art. no. 35201, 2025. DOI: 10.1038/s41598-025-20140-4.